GRADUATE SCHOOL OF OCEANOGRAPHY
UNIVERSITY OF RHODE ISLAND
NARRAGANSETT, RHODE ISLAND

IES Calibration for Main Thermocline Depth: A Method Using Integrated XBT Temperature Profiles

Diagram of Moored IES

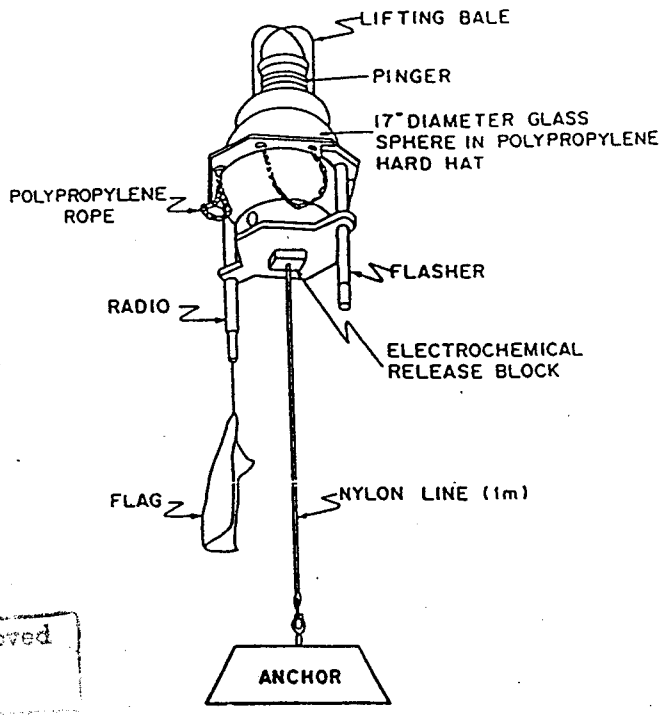

by

S.D. Howden, E. Fields, X. Qian, K. Tracey, and D.R. Watts

GSO Technical Report No. 93-3

November, 1993

This research has been sponsored by the National Science Foundation under grant number OCE87-17144 and by the Office of Naval Research under contract N00014-87-K-0235.

Abstract

A new method of calibrating Inverted Echo Sounder (IES) travel time measurements to main thermocline depths is described. Unlike the traditional method in which the thermocline is defined by a point measurement, such as the depth of the 12°C isotherm depth as measured with an XBT, this technique utilizes the full temperature profile of XBT casts. The advantage of this method is that the vertical integral of temperature, $Q_T = \int T dz$ is conceptually and empirically very closely correlated with the acoustic travel time measured by the IES, $\tau = 2 \int c^{-1} dz$. Comparisons of the new method with the more traditional point method show that the root-mean-square error in the calibration (11 m standard deviation) is $\frac{1}{3}$ as large as before, and outlier values are significantly reduced. The final coefficients used to calibrate the SYNOP Central and Inlet Array IESs are tabulated.

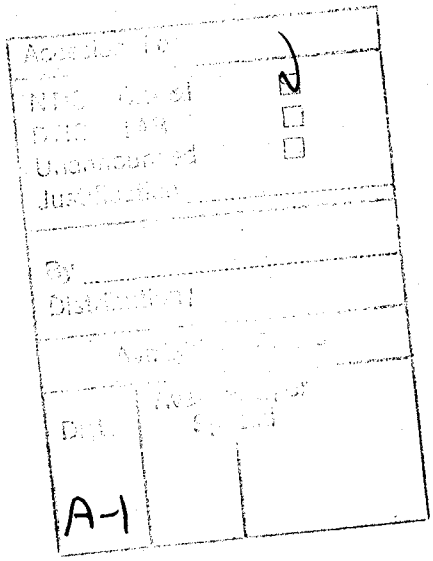

Contents

List of Figures

List of Tables

1 Introduction

An IES measures the time it takes for an emitted acoustic pulse to travel to the sea surface, be reflected and return to the instrument on the ocean floor. From hydrographic data Rossby (1969) showed that, in an appropriate region, the round-trip travel time (τ) measured by an IES is linearly related to the depth of the main thermocline.

Although the main thermocline is defined by a region in the vertical, it is useful for various analyses to characterize it by a single criterion. The most intuitive characterizations are perhaps the depth where the temperature gradient is largest or the midpoint of a depth range defined by a certain value of the gradient. However, these characterizations are not the most convenient ones to implement. We have chosen, for our work in the Gulf Stream, to characterize the thermocline depth as the depth of the 12°C isotherm (Z_{12}) (Friedlander et al., 1986 and Watts et al., 1989), since it is always found in the high gradient region of the Gulf Stream thermal front and does not normally rise to the sea surface at the northern side, even in winter.

In order to convert the round-trip travel time into a thermocline depth a calibration is necessary. As previously mentioned, τ and the main thermocline depth are linearly related. Insofar as Z_{12} represents the main thermocline depth, τ and Z_{12} are also linearly related. The calibration then consists in determining the coefficients (A and B) in the equation

$$Z_{12} = A \cdot \tau + B. \tag{1}$$

In a geographic area where the above linear relation holds, the slope A will have a fixed value for all IESs while the coefficient B will vary depending upon how deep an IES is moored.

In the past, the calibration of an IES had been accomplished by using Z_{12}s measured from XBT casts (calibration XBTs) over the IES site in conjunction with the τ values from the recovered IES data tape. The τ values chosen were the ones which were most nearly coincident in time with the launch of the XBT. Once the slope A of the relationship between Z_{12} and τ had been found, the calibration of each IES was determined by calculating its unique B-intercept (hereafter BINT) which was taken to be the average of the N BINTs calculated from the N XBT casts and coincident τs at that IES site. Thus, for the ith IES:

$$Old\,Method: \quad BINT_i = N^{-1} \cdot \sum_{j=1}^{N} (Z_{12_j} - A \cdot \tau_j) \tag{2}$$

Figure 1a is a flow chart of this process.

Within the main thermocline region the vertical distances between isotherms are compressed or expanded by small scale or high frequency processes such as internal waves. In general, these isotherm depth changes in the thermocline are of small vertical scale. Thus, the individual isotherms can be perturbed in the vertical without a corresponding perturbation of the depth of the thermocline. It is evident that a point measurement, such as the depth of Z_{12} as measured from an XBT cast, is a poorer measure of the thermocline depth than a measurement which uses the full thermal structure of the thermocline. A better characterization of the depth of the main thermocline is then "the average Z_{12}" (Z^*_{12}) for a given value of a water-column integrated quantity which is sensitive to thermocline depth changes. In this way small vertical scale processes are averaged out. Indeed, the Z_{12} value converted from an IES τ record is a sort of Z^*_{12} for the given τ value, because the sound travels through the whole water column. In the past a possible random offset had been introduced for each XBT by using Z_{12} instead of Z^*_{12} in the calibration process. In order to use Z^*_{12} for IES calibrations, we needed to develop a method to estimate it from an XBT cast.

Watts and Rossby (1977) showed that the heat content of a column of water (Q_h) was linearly related to the depth of the main thermocline. Although Q_h cannot be measured with an XBT, the vertically integrated temperature (Q_T) can be measured. If the heat capacity of the column of water is roughly constant, then Q_T is proportional to Q_h and hence should also vary linearly with the thermocline depth. The main subject of this report is a method devised whereby Q_T calculated from an XBT cast can be related to Z^*_{12}. The Q_T used is not linearly related to the depth of the main thermocline since the integration is not done over the entire water column, but rather it is done over a more limited range of depth as dictated by the use of depth limited XBTs. The relationship between Q_T and Z^*_{12} is, however, monotonic so that each Q_T defines a unique Z^*_{12}. Thus, from an XBT cast we can calculate Q_T and convert it into a characteristic depth Z^*_{12}.

The new method was put into practice in a series of steps. The first step was to determine the functional relationship between the thermocline depth and heat content. To do this, the two quantities Z_{12} and Q_T were calculated from a large set of XBT casts in our study region. The limits of integration for Q_T were chosen so that the shallow limit (200 m) would exclude effects in the seasonally forced upper layer and the deep limit (750 m) would include

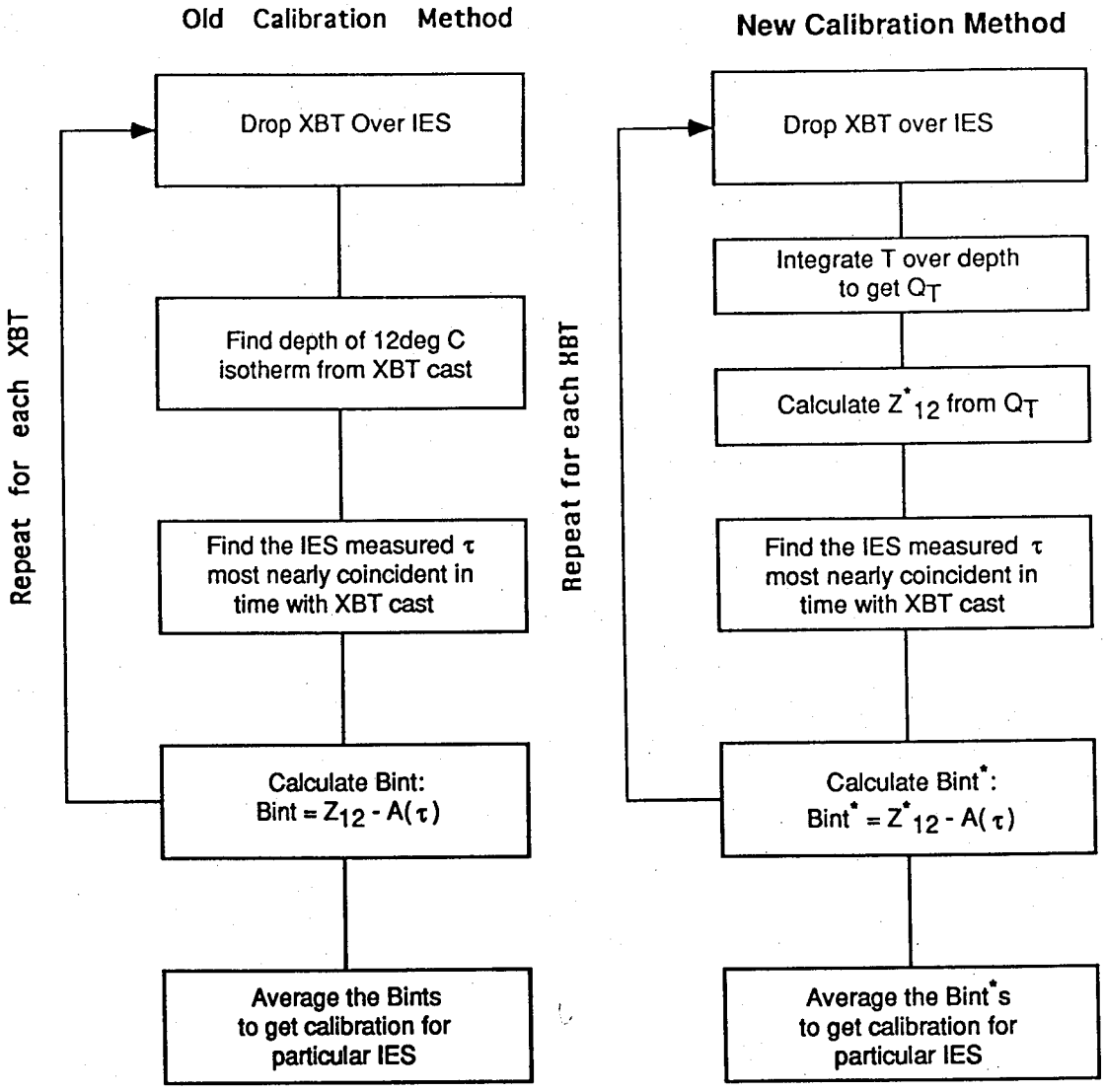

Figure 1a: Flow chart of old method of calibrating IESs.

Figure 1b: Flow chart of new method of calibrating IESs.

typical XBT cast depths. From this large set of data, a functional relationship between Z_{12}^* and Q_T could be determined. The value calculated from this function should then be the desired Z_{12}^* for the water column. In this way Z_{12}^* rather than Z_{12} could be used in the calibration. Thus, with the new method:

$$New\ Method: \quad BINT_i^* = N^{-1} \cdot \sum_{j=1}^{N} (Z_{12\ j}^* - A \cdot \tau_j) \tag{3}$$

Figure 1b is a flow chart of the new calibration process.

2 Data Set

The data used in this study were all collected from XBT casts and IES records from the Central and Inlet Array regions of the SYNOP (Synoptic Ocean Prediction) program. The IES data are described in Qian et al. (1990), Fields and Watts (1990), and Fields and Watts (1991). The times and dates, as well as the locations, of the XBT casts are documented in the SYNOP cruise reports (Friedlander, 1987; Kim, 1988; Fields, 1989; Kim, 1989; Cronin, 1990). The data were used in two different ways. 739 XBT casts, taken in the vicinity of the SYNOP Central Array, were used to determine the functional relationship between Z_{12}^* and Q_T in our region of interest. The XBT drop locations are shown in Figure 2. The IES records and all of the calibration XBT casts (those XBT casts taken near the IES sites) were then used to calibrate the IESs.

There were 9 IES sites in the SYNOP Inlet Array. The sites were arranged in three lines set perpendicular to the mean Gulf Stream path. The SYNOP Central Array consisted of 24 IES sites arranged in 5 lines, again set perpendicular to the mean Gulf Stream path. Figure 3 shows the deployment positions of the IESs in both arrays. Over the three year period 1987–90 IESs were deployed and recovered on an annual basis at up to 33 sites (there was one exception when an IES was not recovered for approximately two years).

Altogether there were 88 IES records for the three deployments. During the three SYNOP IES deployments, a total of 355 calibration XBTs with usable records were dropped at the IES sites.

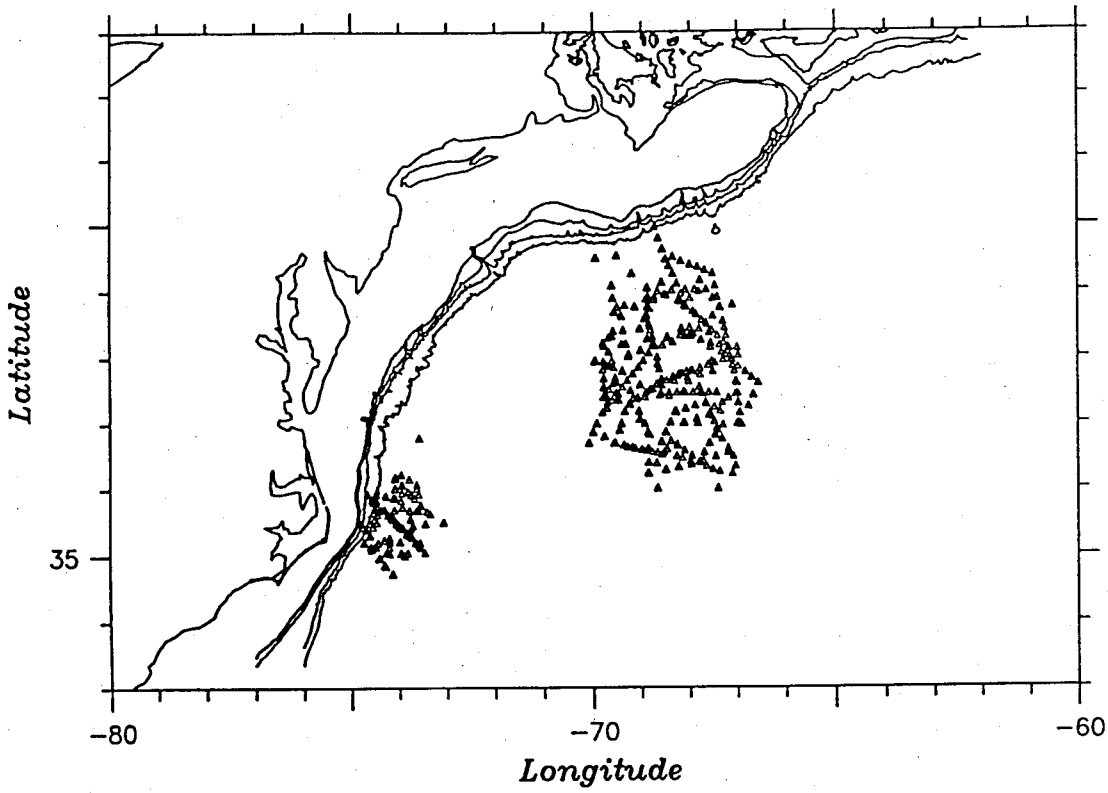

Figure 2: Geographic coverage of XBT casts in the SYNOP Central and Inlet Arrays. Each △ denotes a cast.

3 Z_{12}^* from Q_T

Q_T was defined as

$$Q_T = \int_{200m}^{750m} T dz \tag{4}$$

Excluding the upper 200 m effectively eliminated variability due to the seasonal signal, and the 750 m limit ensured that most T7 XBTs could be used as calibration XBTs. Figure 4 shows the scatter plot of Z_{12} versus Q_T for the SYNOP XBTs.

Superimposed on this plot is the best fit curve to the data, defined as:

$$\begin{aligned} Z_{12}^* &= \underbrace{A1 * exp\{(Q_T - Q1)/\lambda_1\} + A2 * exp\{(Q2 - Q_T)/\lambda_2\}}_{\mathbf{A}} \\ &\quad \underbrace{+a * Q_T + b}_{\mathbf{B}} \end{aligned} \tag{5}$$

The linear part of equation 5 (B) was first determined by fitting a cubic polynomial, using least-squares criteria, to the total SYNOP Central and Inlet Arrays XBT data and then determining the tangent line with the smallest slope. The exponential part of equation 5 (A) was fit to the data after the linear trend was removed. $Q1$ and $Q2$ were fixed and the other coefficients were found by a least-squares fit of the function to the detrended data.

(Note that a different choice of $Q1$ and $Q2$ can be exactly compensated by coefficients $A1$ and $A2$ for the same λs.) The scatter about this curve should be due primarily to variations of the point values of Z_{12} for a particular thermocline depth. Equation 5 has the following coefficients:

$$
\begin{aligned}
Q1 &= 9998 \\
Q2 &= 2912 \\
A1 &= 246.8 \\
A2 &= -107.2 \\
\lambda_1 &= 918.5 \\
\lambda_2 &= 904.5 \\
a &= 0.0788 \\
b &= -65.93
\end{aligned}
$$

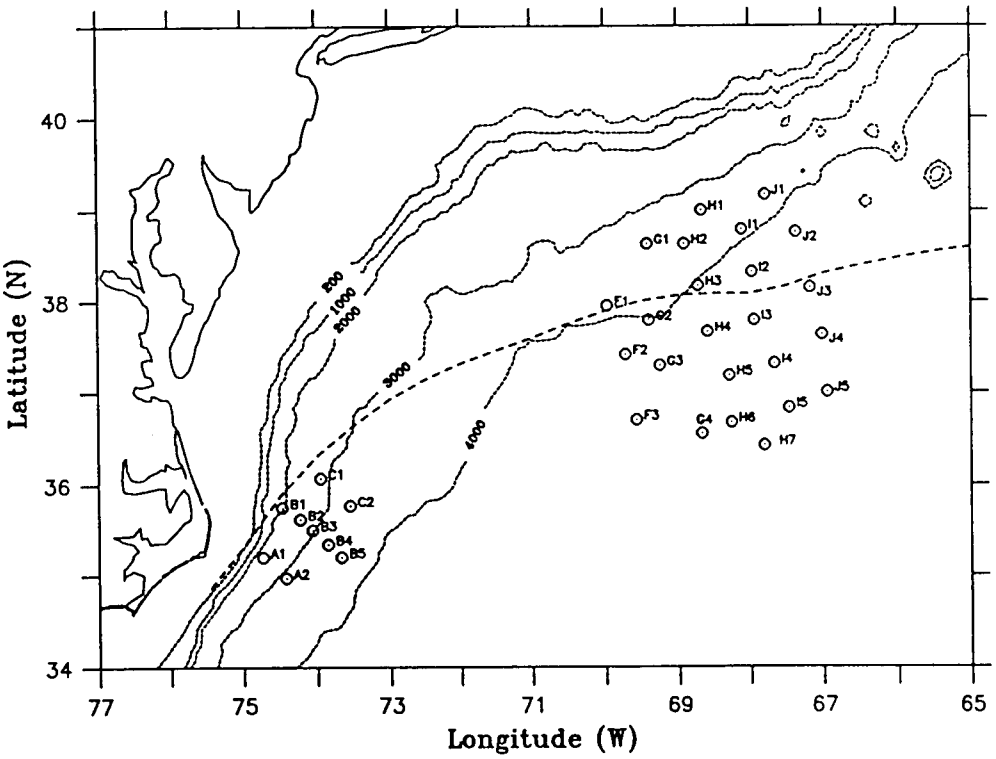

Figure 3: Geographic locations and site names of IESs in the SYNOP Central and Inlet arrays. The dashed line indicates the 12 year mean Gulf Stream sea-surface temperature front (provided by Cornillon, personal communication)

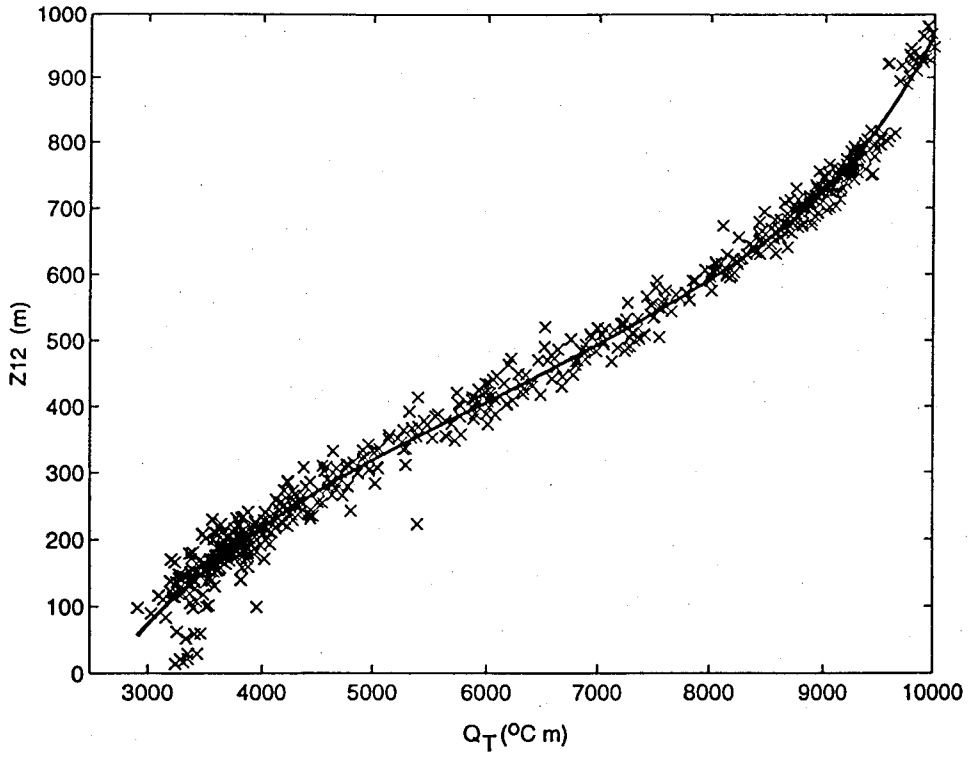

Figure 4: Z_{12} versus $Q_T = \int T dz$ from the SYNOP XBT casts. Superimposed is the best fit curve defined in equation 5.

4 Best Slope

Z^*_{12} still has a linear relationship with travel time τ, but we will see there is less scatter because they are both integral measurements. In order to determine the slope of the 'best straight line' relationship between Z^*_{12} and τ, the sets of $\{Z^*_{12}, \tau\}$ (one set for each IES), from the calibration XBTs and the IESs respectively, were translated to the same line. This was accomplished by subtracting the average Z^*_{12} and τ for each set from the individual values of Z^*_{12} and τ values of the same set. The residual Z^*_{12}s and τs all lie on a straight line which passes through the origin. The residual Z^*_{12}s and τs are defined as:

$$Residual\ Z^*_{12\ i,j} = Z^*_{12\ i,j} - N_j^{-1} \cdot \sum_{i=1}^{N_j} Z^*_{12\ i,j} \tag{6}$$

$$Residual\ \tau_{i,j} = \tau_{i,j} - N_j^{-1} \cdot \sum_{i=1}^{N_j} \tau_{i,j} \tag{7}$$

where $i = 1, N_j$ refers to the ith calibration XBT at the jth IES site. This process allowed a best fit to the entire SYNOP data set, to refine our value of the slope A in Equation 1. The same process was carried out for the sets of $\{Z_{12}, \tau\}$ (the old method) for comparison. Figure 5 shows the scatter plots of both the residual Z^*_{12} and residual Z_{12} versus residual τ

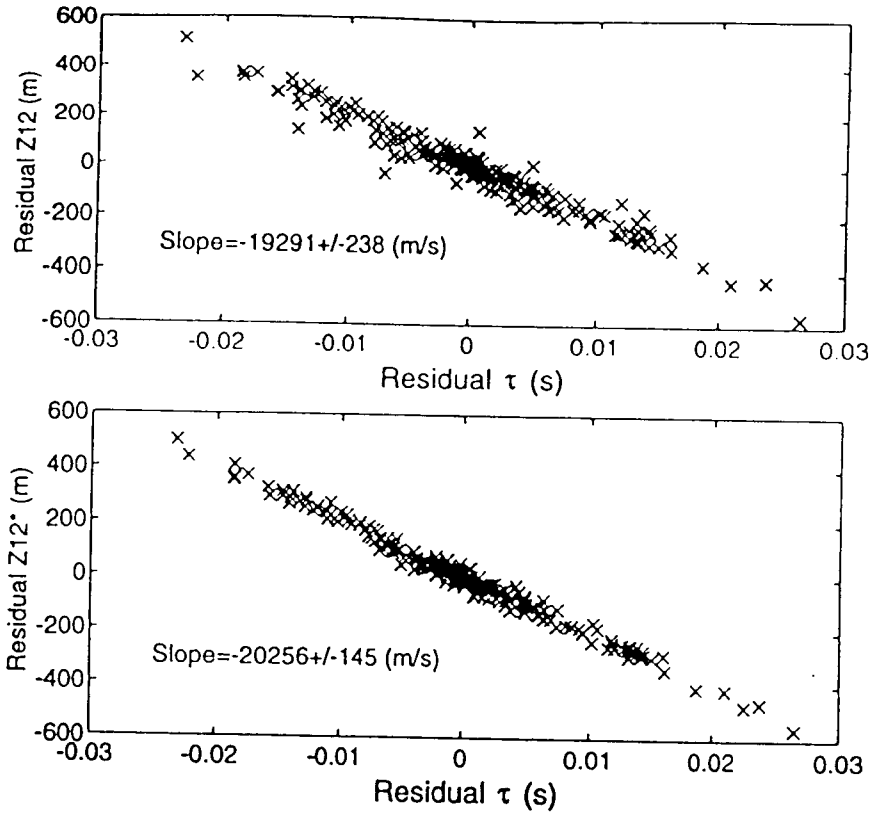

Figure 5: The top panel is a scatter plot of residual Z_{12} versus residual τ (see text for explaination). Also shown is the slope of the linear least-squares best fit to the data. The bottom panel is the same as the top with Z_{12}^* replacing Z_{12}.

and Table 1 lists the results from the linear regressions.

5 B-intercepts

5.1 B-intercepts from Calibration XBTs Only

Tables 2–4 contain the $\overline{BINT}$s and $\overline{BINT^*}$s for all the IESs in the SYNOP Central and Inlet Arrays. Each value is an average over the number of calibration XBTs at that particular site and has an associated standard deviation which is also listed in the tables.

	Old Method	New Method
Slope (ms^{-1})	-19291	-20256
rms error (m)	33	20
St.Dev. (ms^{-1})	238.4	145
R^2(adj)	95.1	98.3

Table 1: Comparison of calibration slope calculated by the old and new methods.

1989-90 Central Array					
IES	$\overline{BINT}$	STDEV	$\overline{BINT^*}$	STDEV*	Final BINT
F1	8427	3	8406	20	8403
F2	1548	29	1538	13	1540
G1	1854	4	1851	15	1851
G2	4644	23	4645	5	4645
G3	4720	50	4759	15	4759
G4	5879	37	5851	29	5853
H1	7174	33	7173	17	7173
H2	4553	5	4552	15	4557
H3	3605	16	3613	13	3614
H4	7087	61	7102	19	7088
H5	8774	156	8876	33	8876
H6	2252	41	2243	27	2253
H7	3270	32	3241	9	3241
I1	6255	†	6259	†	6255
I2	1927	22	1927	10	1927
I3	3229	17	3243	21	3239
I4	8096	86	8134	19	8140
I5	4547	35	4547	28	4547
J1	5252	53	5270	18	5270
J2	2194	24	2183	23	2183
J3	3536	44	3531	33	3534
J4	2228	34	2249	38	2270
J5	5062	23	5053	18	5053

1989-90 Inlet Array					
IES	$\overline{BINT}$	STDEV	$\overline{BINT^*}$	STDEV*	FINAL BINT
A1	3516	40	3475	11	3475
A2	2540	9	2532	13	2532
B1	4798	18	4770	36	4770
B3	7685	38	7688	24	7688
B4	1818	33	1809	26	1809
B5	1828	22	1826	19	1826
C1	4423	25	4406	30	4406
C22	4811	48	4812	30	4812
C21	5037	23	5038	13	5038

Table 2: BINTs and BINT*s, and corresponding standard deviations for the IESs in the 1989-90 SYNOP Central and Inlet Arrays. The † indicates that the standard deviation was undefined because only one calibration XBT was available.

1988-89 Central Array					
IES	$\overline{BINT}$	STDEV	$\overline{BINT^*}$	STDEV*	FINAL BINT
F1	8452	5	8461	25	8461
F2	1575	24	1561	8	1561
F3	6286	37	6306	12	6306
G1	2008	10	2015	9	2008
G2	4639	28	4642	20	4642
G3	4655	19	4668	37	4680
G4	5703	93	5784	24	5784
H1	7154	25	7191	6	7191
H2	8100	17	8086	6	8086
H3	3619	28	3629	23	3613
H4	7025	13	7014	8	7000
H5	8806	11	8802	28	8790
H6	1960	88	2039	18	2045
H71	3164	154	3301	26	3310
H72	3325	10	3320	1	3320
I1	6316	0	6311	4	6311
I2	1402	24	1401	15	1385
I4	8090	17	8099	26	8088
I5	4376	36	4465	18	4460
J1	5232	49	5285	8	5285
J2	2081	25	2075	39	2082
J3	3879	18	3877	11	3865
J4	2276	29	2277	35	2277
J5	4989	2	5003	24	5003

1988-89 Inlet Array					
IES	$\overline{BINT}$	STDEV	$\overline{BINT^*}$	STDEV*	FINAL BINT
B1	4679	20	4665	18	4665
B2	7547	35	7567	28	7567
B3	8394	19	8414	16	8414
B41	1733	41	1733	31	1733
B42	1804	9	1803	2	1803
B51	1943	44	1952	37	1952
B52	1862	20	1861	8	1861
C1	4278	34	4293	7	4293
C2	4629	7	4639	6	4639

Table 3: BINTs and BINT*s, and corresponding standard deviations for the IESs in the 1988-89 SYNOP Central and Inlet Arrays.

1987-88 Central Array					
IES	$\overline{BINT}$	STDEV	$\overline{BINT^*}$	STDEV*	FINAL BINT
G2	8465	12	8466	11	8466
G3	4092	10	4090	10	4090
G4	5361	47	5394	20	5394
G5	2746	55	2790	22	2790
H2	5476	32	5491	12	5491
H3	2275	14	2292	7	2292
H4	2468	24	2469	28	2469
H5	1111	58	1188	43	1188
I1	1030	33	1035	36	1035
I2	4802	16	4807	16	4807
I3	6478	24	6490	18	6490
I4	3748	24	3752	19	3752
I5	5600	77	5673	2	5673

1987-88 Inlet Array					
IES	$\overline{BINT}$	STDEV	$\overline{BINT^*}$	STDEV*	FINAL BINT
A1	2655	11	2661	29	2661
A2	4215	25	4221	28	4221
B1	4791	23	4780	27	4780
B2	7809	16	7814	15	7814
B3	8434	26	8432	17	8432
B4	1768	28	1774	30	1774
B51	1814	20	1829	57	1829
B52	1853	8	1834	8	1834
C1	4246	15	4259	18	4259
C2	4685	23	4683	19	4683

Table 4: BINTs and BINT*s, and corresponding standard deviations for the IESs in the 1987-88 SYNOP Central and Inlet Arrays.

Figures 6 and 7 show histograms of the standard deviations. For comparison, Figure 6 is a histogram of the standard deviations of the BINTs, the B-intercepts calculated using the old calibration method, whereas Figure 7 shows those obtained with the new method. Note that the center of the distribution for the old method has a greater value than that of the new method. Also, using the old method results in both a greater occurrence and magnitude of outlier values. Table 5 shows the average and standard deviations for the two distributions.

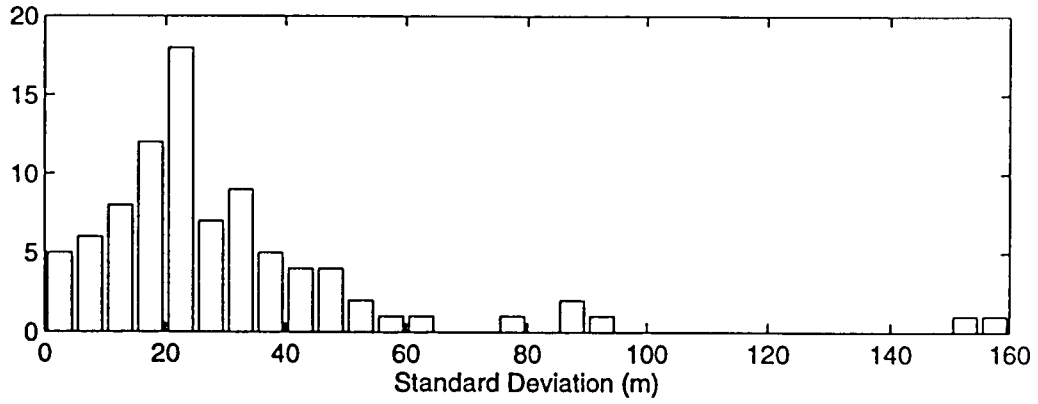

Figure 6: Histogram of the standard deviations for all BINTs. Each "count" is the standard deviation of the set of BINTs for a particular IES.

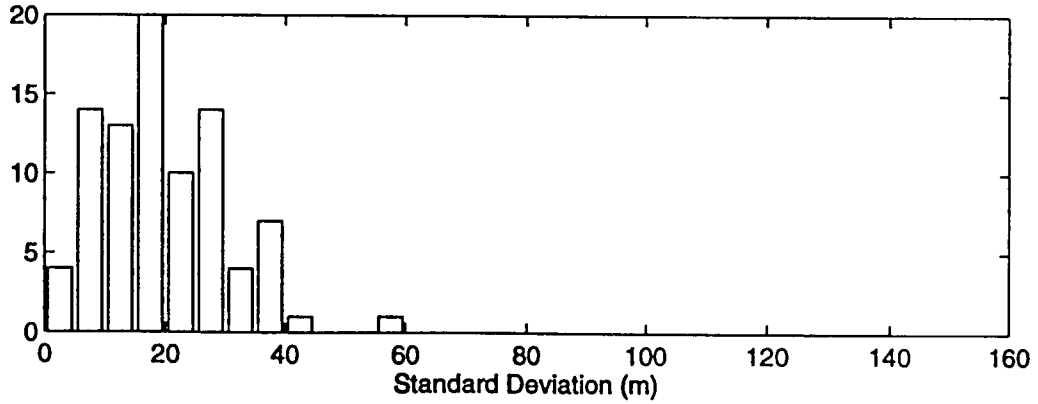

Figure 7: Histogram of the standard deviations for all BINT*s. Each "count" is the standard deviation of the set of BINT*s for a particular IES.

	New Method	Old Method
Average (m)	19.7	30.9
σ (m)	10.7	26.5

Table 5: Standard deviations and averages of the sets of standard deviations for the BINTs and BINT*s.

5.2 Final B-intercepts for SYNOP Central and Inlet Array IESs

The preceeding sections described the new method used to determine the calibration coefficients for IESs. In this section we document how the SYNOP IES calibrations were further improved by taking into account additional measurements of the thermocline depth obtained from other data sources in the study region. These sources included (i) all XBTs taken on the IES deployment and recovery cruises but were not located right at the instrument sites, (ii) all XBTs located within the Central Array that were dropped as part of the Gulf Stream Anatomy experiment (Hummon et al., 1991), and (iii) twelve current meter moorings located in the Central Array. The adjusted BINT*s, tabulated below, were used in the final calibration of the SYNOP IES.

XBTs. For each XBT, we determined Z^*_{12} using the method described previously. However, because these XBTs were not dropped directly over the IES sites, their Z^*_{12} values could not be used in conjunction with coincident τ measurements to determine BINT*s. Therefore, an alternate approach was developed in order to incorporate these XBTs into the calibration process. The first step was to calibrate the IES τ measurements into Z^*_{12} using the BINTs listed in Tables 2–4. Then, objective maps of these Z^*_{12} estimates were made using the techniques described in Tracey and Watts (1991). The second step was to interpolate the maps to find the Z^*_{12} value at the position and time of each XBT drop. Subsequently the differences ΔZ^*_{12} between the IES-derived and XBT Z^*_{12} estimates were calculated.

Current Meters. The moorings in the SYNOP Central Array consisted of 4 current meters at nominal depths of 400, 700, 1000, and 3500 m. Because these tall moorings were pulled over by the drag of the current, the temperature and velocity measurements were corrected for mooring motion as described in Cronin et al. (1992). A by-product of this motion compensation procedure was a time series of the pressure of the 12°C isotherm at each site. These pressures in decibars were scaled by 1.01 to obtain records of depth in

meters, which are identical to the IES Z_{12}^* measurements. The current meter and IES Z_{12}^* values were compared by first interpolating the IES-derived objective maps to each current meter site and then calculating the record-long averages of the differences (ΔZ_{12}^*).

*Adjustment of BINT**. We used the XBT and current meter ΔZ_{12}^* values to adjust the BINT*s of the IESs. This was accomplished by treating each ΔZ_{12}^* as a supplementary calibration XBT; thus the BINTs listed in Tables 2–4 were adjusted either upwards or downwards by weighting each ΔZ_{12}^* according to the total number of calibration XBTs at each IES. The final BINT*s used to calibrate the SYNOP IESs are listed in Tables 6 and 7.

6 Summary

From a relatively large and well scrutinized data set (over 700 XBTs), a functional relationship between the temperature integrated over standard depth limits Q_T and the depth of the 12°C isotherm was found. The scatter about this best fit curve is primarily due to the scatter of the point measurement of Z_{12} about a given thermocline depth. This function then allows a quantity Z_{12}^*, with a tighter linear relation to the thermocline depth than Z_{12}, to be calculated from an XBT cast via the Q_T calculation.

The use of Z_{12}^*, rather than Z_{12}, improves the calibration of IESs in two ways. It improves both the relative measure of the thermocline depth, i.e., the measurement at one time relative to that at another at each IES site, and the absolute value of the thermocline depth. The improvement in the relative measure of the thermocline depth is due to the factor of two improvement in the standard deviation of the determination of the slope A. The improvement in the absolute measure of the thermocline depth is indicated by the reduction by a factor of four of the standard deviation of the distribution of standard deviations for the BINT*s versus that of the BINTs.

SYNOP Central Array					
1987–1988		1988–1989		1989–1990	
IES	FINAL BINT*	IES	FINAL BINT*	IES	FINAL BINT*
		F1	8461	F1	8403
		F2	1561	F2	1540
		F3	6306		
		G1	2008	G1	1851
G2	8466	G2	4642	G2	4645
G3	4090	G3	4680	G3	4759
G4	5394	G4	5784	G4	5853
G5	2790				
		H1	7191	H1	7173
H2	5491	H2	8086	H2	4557
H3	2292	H3	3613	H3	3614
H4	2469	H4	7000	H4	7088
H5	1188	H5	8790	H5	8876
		H6	2045	H6	2253
		H71	3310	H7	3241
		H72	3320		
I1	1035	I1	6311	I1	6255
I2	4807	I2	1385	I2	1927
I3	6490			I3	3239
I4	3752	I4	8088	I4	8140
I5	5673	I5	4460	I5	4547
		J1	5285	J1	5270
		J2	2082	J2	2183
		J3	3865	J3	3534
		J4	2277	J4	2270
		J5	5003	J5	5053

Table 6: Final BINT*s used to calibrate the SYNOP Central Array IESs for the three deployment periods spanning 1987–1990.

SYNOP Inlet Array					
1987–1988		1988–1989		1989–1990	
IES	FINAL BINT*	IES	FINAL BINT*	IES	FINAL BINT*
A1	2661			A1	3475
A2	1561			A2	2532
B1	4780	B1	4665	B1	4770
B2	7814	B2	7567	B2	7688
B3	8432	B3	8414	B3	1809
B4	1774	B41	1733	B4	1826
		B42	1803		
B51	1829	B51	1952	B5	
B52	1834	B52	1861		
C1	4259	C1	4293	C1	4406
C2	4683	C2	4639	C22	4812
				C21	5038

Table 7: Final BINT*s used to calibrate the SYNOP Inlet Array IESs for three deployment periods spanning 1987–1990.

7 References

Cronin, M., *Data report for cruise EN216.* Cruise Report, University of Rhode Island, Narragansett, Rhode Island, 1990, 41 pp.

Cronin, M, K. L.Tracey, and D.R. Watts, *Mooring motion correction of SYNOP Central Array current meter data.* GSO Technical Report No. 92–4, University of Rhode Island, Narragansett Rhode Island, 1992, 114 pp.

Fields, E., *Data report for cruise OC207.* Cruise Report, University of Rhode Island, Narragansett, Rhode Island, 1989, 50 pp.

Fields, E. and D.R. Watts, *The SYNOP experiment: inverted echo sounder data report for May 1988 to August 1989.* GSO Technical Report No. 90–2, University of Rhode Island, Narragansett, Rhode Island, 1990, 232 pp.

Fields, E. and D.R. Watts, *The SYNOP experiment: inverted echo sounder data report for June 1989 to September 1990.* GSO Technical Report No. 91–2, University of Rhode Island, Narragansett, Rhode Island, 1991, 255 pp.

Friedlander, A.I., K.L. Tracey and D.R. Watts, *The Gulf Stream Dynamics Experiment: inverted echo sounder data report for the July 1982 to April 1983 deployment period.* GSO Technical Report No. 86–5, University of Rhode Island, Narragansett, Rhode Island, 1986, 101 pp.

Friedlander, A.I., *Data report for cruise EN169.* Cruise Report, University of Rhode Island, Narragansett, Rhode Island, 1987,60 pp.

Hummon, J., T.Rossby, E. Carter, J. Lillibridge, M. Liu, K. Schultz Tokos, S. Anderson-Fontana, and A. Mariano, *The Anatomy of Gulf Stream meanders.* GSO Technical Report No. 91–4 *Volumes 1 and 2.*, University of Rhode Island, Narragansett, Rhode Island, 1991.

Kim, H.-S., *Data report for cruise OC200.* Cruise Report, University of Rhode Island, Narragansett, Rhode Island, 1988, 34 pp.

Kim, H.-S., *Data report for cruise OC210.* Cruise Report, University of Rhode Island, Narragansett, Rhode Island, 1989, 27 pp.

Qian, X., K.L. Tracey, and D.R. Watts, *The SYNOP experiment: inverted echo sounder data report for October 1987 to May 1988.*, GSO Technical Report No. 90-3, University of Rhode Island, Narragansett, Rhode Island, 1990, 156 pp.

Rossby, H.T., On monitoring depth variations of the main thermocline acoustically. *J. Geophys. Res.*, 74, 5542–5546, 1969.

Tracey, K.L., and D. R. Watts, *The SYNOP experiment: Thermocline depth maps for the Central Array October 1987 to August 1990.* GSO Technical Report No. 91-5, 1991, 193 pp.

Watts, D.R. and H.T. Rossby, Measuring dynamic heights with inverted echo sounders: results from MODE. *J. Phys. Oceanogr.*, 7, 346–358, 1977.

Watts, D.R., K.L. Tracey, and A.I. Friedlander, Producing accurate maps of the Gulf Stream thermal front using objective analysis. *J. Geophys. Res.*, 94, 8040–8052, 1989.

SECURITY CLASSIFICATION OF THIS PAGE

REPORT DOCUMENTATION PAGE

1a. REPORT SECURITY CLASSIFICATION Unclassified	1b. RESTRICTIVE MARKINGS
2a. SECURITY CLASSIFICATION AUTHORITY	3. DISTRIBUTION / AVAILABILITY OF REPORT Distribution for public release; Distribution is unlimited.
2b. DECLASSIFICATION / DOWNGRADING SCHEDULE	
4. PERFORMING ORGANIZATION REPORT NUMBER(S) University of Rhode Island Graduate School of Oceanography GSO Technical Report 93-3	5. MONITORING ORGANIZATION REPORT NUMBER(S)
6a. NAME OF PERFORMING ORGANIZATION University of Rhode Island Graduate School of Oceanography 6b. OFFICE SYMBOL (If applicable) 1122 PO	7a. NAME OF MONITORING ORGANIZATION
6c. ADDRESS (City, State, and ZIP Code) South Ferry Road Narragansett, RI 02882-1197	7b. ADDRESS (City, State, and ZIP Code)
8a. NAME OF FUNDING / SPONSORING ORGANIZATION Office of Naval Research National Science Foundation 8b. OFFICE SYMBOL (If applicable)	9. PROCUREMENT INSTRUMENT IDENTIFICATION NUMBER N00014-87-K-0235; OCE87-17144
8c. ADDRESS (City, State, and ZIP Code) 800 N. Quincy Street, Arlington, VA 22217 4201 Wilson Boulevard, Arlington, VA 22230	10. SOURCE OF FUNDING NUMBERS PROGRAM ELEMENT NO. / PROJECT NO. / TASK NO. / WORK UNIT ACCESSION NO.

11. TITLE (Include Security Classification)
IES Calibration for Main Thermocline Depth: A Method Using Integrated XBT Temperature Profiles

12. PERSONAL AUTHOR(S)
S.D. Howden, E. Fields, X. Qian, K. Tracey and D.R. Watts

13a. TYPE OF REPORT	13b. TIME COVERED	14. DATE OF REPORT (Year, Month, Day)	15. PAGE COUNT
Summary	FROM 5/88 TO 8/90	November 1993	21

16. SUPPLEMENTARY NOTATION

17. COSATI CODES			18. SUBJECT TERMS (Continue on reverse if necessary and identify by block number)
FIELD	GROUP	SUB-GROUP	Gulf Stream, SYNOP, Inverted Echo Sounder Calibration

19. ABSTRACT (Continue on reverse if necessary and identify by block number)

A new method of calibrating Inverted Echo Sounder (IES) travel time measurements to main thermocline depths is described. Unlike the traditional method in which the thermocline is defined by a point measurement, such as the depth of the 12°C isotherm depth as measured with an XBT, this technique utilizes the full temperature profile of XBT casts. The advantage of this method is that the vertical integral of temperature, $Q_T = \int T dz$ is conceptually and empirically very closely correlated with the acoustic travel time measured by the IES, $\tau = 2 \int c^{-1} dz$. Comparisons of the new method with the more traditional point method show that the root-mean-square error in the calibration (11 m standard deviation) is $\frac{1}{3}$ as large as before, and outlier values are significantly reduced. The final coefficients used to calibrate the SYNOP Central and Inlet Array IESs are tabulated.

20. DISTRIBUTION / AVAILABILITY OF ABSTRACT ☒ UNCLASSIFIED/UNLIMITED ☐ SAME AS RPT. ☐ DTIC USERS	21. ABSTRACT SECURITY CLASSIFICATION
22a. NAME OF RESPONSIBLE INDIVIDUAL D. Randolph Watts	22b. TELEPHONE (Include Area Code) / 22c. OFFICE SYMBOL

DD FORM 1473, 84 MAR 83 APR edition may be used until exhausted. All other editions are obsolete.

SECURITY CLASSIFICATION OF THIS PAGE